# Electron–Hole Plasma-Induced Spectral Blueshift of Optical-Data Injection Mode-Locked Semiconductor Optical Amplifier Fiber Laser

Gong-Ru Lin, *Senior Member, IEEE*, Yu-Chan Lin, Kuen-Cherng Lin, and Guo-Hsuan Peng

***Abstract*—Under an optical nonreturn-to-zero (NRZ) data injection at 10 Gbit/s, the 10-GHz mode-locking and pulsed return-to-zero (RZ) clock extraction from a semiconductor optical amplifier (SOA) based fiber ring is investigated in this paper. The diagnoses on gain and intracavity-power-controlled anomalous blueshifted spectrum and subpicosecond timing jitter are demonstrated. By increasing the injecting power of the optical NRZ data from −3 to 8 dBm into the SOA bias at different currents, the mode locking is completed with a dc level greatly decreasing from 480 to 50 $\mu$W (only 1.5% of the mode-locked pulse power at 3 mW), corresponding to a pulse/dc amplitude contrast ratio up to 18 dB. Increasing the SOA bias current up to 350 mA significantly suppresses the timing jitter from 1.8 ps to 345 fs, and the extracted RZ clock pulse is shortened from 55 to 27 ps. The pulsewidth of the amplified SOAFL is compressed from 11 ps to 836 fs after dispersion compensation. At constant data injection level, the increasing SOA bias or gain oppositely redshifts the mode-locked SOA fiber ring laser (SOAFL) spectrum by 5 nm. The amplifier spontaneous emission of SOA at short wavelength region (∼1520 nm) is eliminated with increasing NRZ data power, whereas the mode-locking gain peak arises and blueshifts from 1558 to 1552 nm due to the band-filling effect. Such a blueshift in mode-locking spectrum becomes more significant in SOA at lower bias (or gain) condition. A theoretical model interprets the correlation between the nonlinear gain suppression-induced variation of electron–hole plasma in SOA and the blueshifted mode-locking SOAFL spectrum, which is occurred when the gain saturation condition for the SOA becomes more pronounced.**

***Index Terms*—Blueshift, fiber lasers, injection mode locking, semiconductor optical amplifier (SOA), spectrum.**

## I. Introduction

Since early years, versatile configurations of ultrafast mode-locking fiber lasers have been developed with their tunable pulsewidth and spectrum meeting the demands for applications in fiber-optic communication and diagnostics [1]–[5]. Among different approaches, the use of intracavity laser diode [1] or amplifier [2] for modulating the gain instead of the loss of the fiber laser has emerged as an intriguing technology for injection mode locking. With the fast development on the high-damage-threshold semiconductor optical amplifier (SOA), the new class of the mode-locked SOA fiber ring lasers (SOAFLs) [6], [7], by using techniques such as the active nonlinear polarization rotation [8], the cross-phase modulation [9], and the cross-gain modulation [10], etc., have been introduced in past decade. This type of SOA-based fiber lasers gradually become the alternative to the remarkable schemes of the mode-locked fiber laser sources, such as the actively mode-locked erbium-doped fiber lasers (EDFLs) using laser diode (or amplifier) based intensity modulator and intracavity filter [11], [12], and the mode-locked SOAFLs via the periodical control of the SOA driving current [13], [14].

More recently, the injection of optical data or transistor–-transistor logic (TTL) clock with large duty cycle was demonstrated as the new scheme to extract the optical clock or implement the mode locking in SOAFL [15], [16], respectively. With this approach, Tangdiongga *et al.* have demonstrated a 10 GHz optical clock recovery (OCR) from 160-Gbit/s optical time-division multiplexing (OTDM) data stream. Similar experiment has also been reported for all-optical clock recovery by using mode-locked SOAFL, which is capable of recovering the clock signal from the optical nonreturn-to-zero (NRZ) data stream with bit rate up to 12.5 Gbit/s. The recovered RZ clock pulse train is chirp-free with its timing jitter decreasing to 200 fs [13], [14]. Such an optical-injection mode-locking and clock-recovery scheme could benefit from the advantage from all-optical mode-locking technique, thus relieving the limitation on the direct modulation bandwidth set by the contact electrode of the SOA itself, and provides a higher mode-locking frequency to achieve high-bit-rate optical clock pulse generation for the OTDM networks. Nonetheless, the parametric analyses on the optical injection induced direct gain modulation, mode locking, and data/clock recovery of SOAFL were seldom reported, and the mechanisms responsible for the evolution on gain-saturated SOAFL spectrum under optical clock injection induced mode locking was never discussed even though.

In this paper, we investigate the 10-GHz mode locking and RZ pulsed clock extraction from an SOA-based fiber ring, which is achieved by injecting the optical pseudorandom-bit-sequence (PRBS) NRZ data injection at 10 Gbit/s with changing power levels, and by detuning the bias current of SOA under external injection. The parametric analyses on the DC level, the pulsewidth, the timing jitter, and the pulse amplitude are performed to optimize the recovery of RZ clock pulse. The amplifier and dispersion compensator are employed to compress the SOAFL pulse down to subpicosecond regime. In particular, we employ the electron–hole plasma-induced wavelength-shift

Manuscript received May 20, 2009; revised September 21, 2009. First published November 24, 2009; current version published January 15, 2010. This work was supported in part by the National Science Council under Grant NSC-98-2221-E-002-055.

G.-R. Lin, Y.-C. Lin, and G.-H. Peng are with the Graduate Institute of Photonics and Optoelectronics, and the Department of Electrical Engineering, National Taiwan University, Taipei 106, Taiwan (e-mail: grlin@ntu.edu.tw).

K.-C. Lin is with the Institute of Electro-Mech-Optic Engineering, China Institute of Technology, Taipei 115, Taiwan.

Color versions of one or more of the figures in this paper are available online at http://ieeexplore.ieee.org.

Digital Object Identifier 10.1109/JLT.2009.2036867

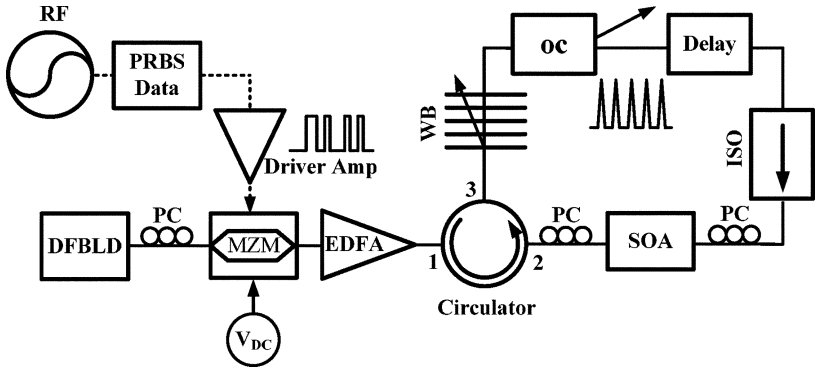


Fig. 1. Experimental setup of the SOAFL. Amp: amplifier, DFBLD: distributed feedback laser diode, EDFA: erbium-doped fiber amplifier, ISO: isolator, MZM: Mach–Zehnder intensity modulator, OC: optical coupler, PC: polarization controller, PRBS data: pseudorandom bit sequence data generator, RF: RF synthesizer, SOA: semiconductor optical amplifier, and WB: wavelength blocker.

model to elucidate the intracavity gain and power-controlled anomalous blueshifted spectrum of the SOAFL-recovered RZ clock pulse.

## II. Experimental Setup

In the experiment, a commercial SOA (Qphotonics, QSOA-1550) was employed as the gain medium inside the fiber ring. The bias current of SOA was detuned from 250 to 350 mA to optimize the mode locking of such an SOAFL. The upper limit of the SOA bias current given by manufacturer is 400 mA. Therefore, we control the maximum SOA bias current at 350 mA in order to prevent the damage of such a device. To inject the SOA, an electrical NRZ data stream with its PRBS pattern length of $2^{31}-1$ and duty cycle enlarged from 50% to 90% was generated from a 10-Gbit/s pattern generator (Hewlett Packard, HP 70843B) driven by a 10-GHz frequency synthesizer (Agilent, E8257C). The NRZ data stream was amplified via a microwave amplifier (JDSU, H301–1110) before driving the Mach–Zehnder intensity modulator (MZM, JDSU, 10024180) bias at a half-wave voltage of $V_\pi = 4.5$ V. The optical injection of 7 dBm at 1555.7 nm was obtained by seeding the DFB laser diode (DFBLD) output through the amplified NRZ-driven MZM at dc bias of $3V_\pi/4$ [19]. The DFBLD was driven at continuous-wave (CW) lasing condition and the external modulation was done using the MZM intensity modulator.

Except the clockwise optical isolator, the output coupler, and the polarization controller, we further introduce a fiber Bragg-grating-based wavelength blocker to terminate the injected optical NRZ data, which maybe clockwise propagated in the fiber ring cavity. The optical NRZ data injection reduces the gain of SOA and provides the narrow gain window in SOA, which initiates the pulsed mode locking of the SOAFL after detuning the NRZ repetition frequency to match the harmonics of the longitudinal mode in the SOAFL cavity. [20] An EDFA with tunable output power of up to 17 dBm is used to detune the NRZ power for injecting the SOAFL, such that an optical signal with extremely large duty cycle is generated to achieve the best ON–OFFextinction ratio of the recovered RZ clock pulse. An intracavity polarization controller (PC) was employed to confirm the maximum power feedback into the polarization-sensitive SOA. To extract the RZ clock pulse from the incoming NRZ data stream at any repetition frequency, an additional true time delay line was added into the fiber ring for optimizing the mode locking performance of the SOAFL. A digital sampling oscilloscope (Agilent, 86100A+86106B) was used to measure the traces and timing jitter of the RZ clock pulse extracted by the mode-locked SOAFL.

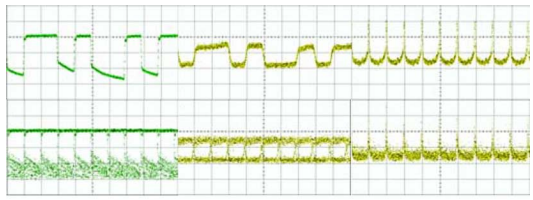


Fig. 2. Shapes (upper part) and eye-diagram (lower part) of (a) the incoming electrical NRZ data stream from a PRBS generator; (b) the optical NRZ data stream after MZM; (c) the mode-locked pulse from SOAFL under optical NRZ injection.

## III. Results and Discussion

### A. Effects of SOA Bias and External NRZ Injection on Mode-Locking SOAFL Pulses

The bit shape and eye diagram of the electrical PRBS NRZ data stream with a pattern length of $2^{23}-1$ employed to modulate the DFBLD are shown in Fig. 2(a). The bit shape and eye diagram of the incoming optical NRZ data stream simulated by externally encoding a DFBLD output with an MZM driven by the PRBS NRZ data stream are shown in Fig. 2(b). In this case, most of the gain in the SOA is temporally depleted under the optical NRZ data injection. With a fine adjustment on the SOAFL ring cavity length via an intracavity delay-line controller, the harmonic longitudinal-mode frequency of the SOAFL is adjusted to match with the frequency of the incoming optical NRZ data stream. As a result, the recovered RZ clock pulse can be generated by optical NRZ injection mode locking the SOAFL, as shown in Fig. 2(c).

By controlling the injecting power of the optical NRZ data stream form $-3$ to 8 dBm, we discuss the pulse/dc levels and corresponding ON–OFFextinction ratios of the recovered RZ clock pulse. In Fig. 3, we have observed that the mode-locking pulse amplitude of SOAFL becomes higher with increasing

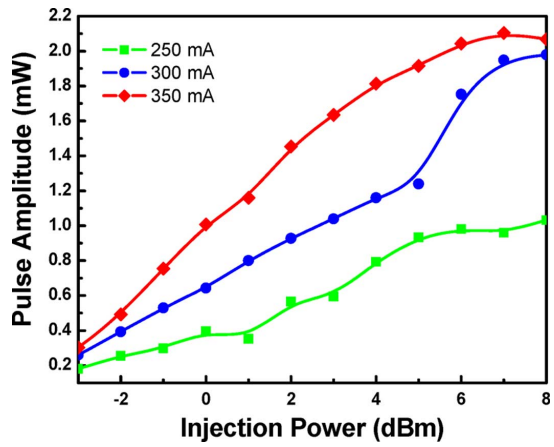


Fig. 3. Injection power-dependent pulse amplitude of mode-locking SOAFL at different biases.

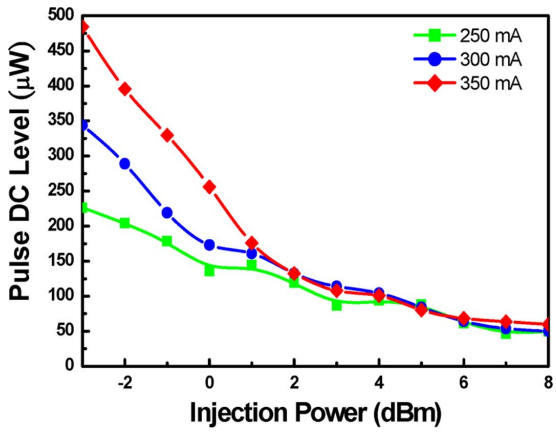


Fig. 4. Injection power-dependent dc level of mode-locking SOAFL at different biases.

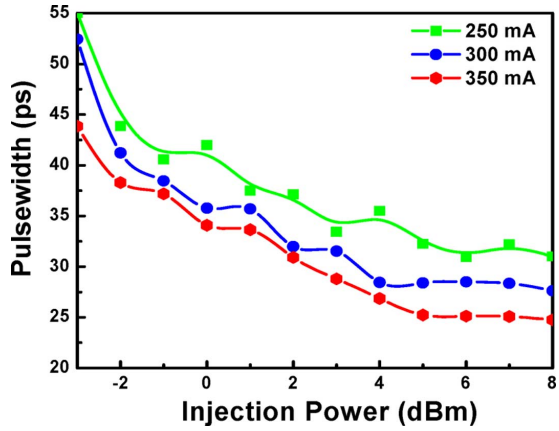


Fig. 5. Injection power-dependent pulsewidth of mode-locking SOAFL at different biases.

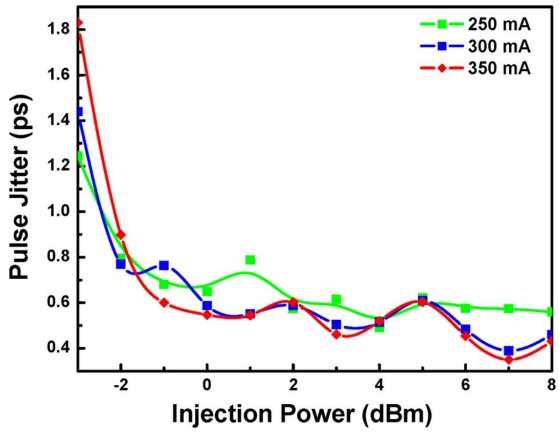


Fig. 6. Injection power-dependent jitter of mode-locking SOAFL at different biases.

bias current of SOA. With increasing power of the optical NRZ injection, the RZ pulse amplitude can be significantly enlarged by one order of magnitude (from 0.2 to 2.0 mW). The output pulse amplitude exhibits a linear proportionality with the optical NRZ injection power, which slightly saturates at higher injecting levels due to the gain saturation phenomenon of SOA. On the other hand, the mode locking is optimized by injecting strong optical NRZ signal and maximize the feedback power into SOA, since the higher feedback power exhausts more gain of SOA to achieve larger modulation depth.

Fig. 4 shows that the dc level accompanied with the mode-locked SOAFL pulse. Apparently, the dc level is greatly decreased with increasing power of the injected optical NRZ data. The stronger NRZ power can deplete more gain to suppress the amplified spontaneous emission (ASE) output from the SOAFL. Therefore, the minimum dc level obtained at different SOA biases is reduced from 480 to 50 $\mu$W (only 1.5% of the mode-locked pulse amplitude) and saturated at 50 $\mu$W at all bias conditions. The gain of SOA will be greatly saturated to reduce the output dc level down to $-14$ dBm, providing an RZ clock pulse with high ON–OFFextinction ratio after extracting from the injected NRZ signal. That is, the mode locking is gradually completed with the decreasing dc level of the output RZ clock pulse, which eventually results in a pulse/dc amplitude contrast ratio up to 18 dB.

In Fig. 5, the pulsewidth of the mode-locking SOAFL is shortened by increasing the NRZ injected power, and we also find that the higher bias current of SOA can essentially promote larger modulation depth after gain depletion to make shorter pulsewidth. Under the injection of 10-Gbit/s NRZ data, the mode-locking SOAFL pulsewidth can be shortened from 55 to 27 ps with an average power of 3 mW. The strong injection and enlarged bias current makes the pulsewidth narrower than the case of weak injection and the small bias. The ASE component in the SOA is suppressed as the dc level is effectively reduced, such that the timing jitters are concurrently reduced by increasing the injection power, as shown in Fig. 6.

By using the strong optical NRZ injection, we can confirm that the gain medium (SOA) only provides sufficient gain to the mode-locking laser (SOAFL) within in a limited temporal window. However, the ASE–ASE beating noise becomes significant, and inevitably causes large phase noise as well as timing jitter as the SOA bias increases. At low power level of optical NRZ data injection, the timing jitter of the mode-locked SOAFL keeps as high as 1.8 ps. By increasing SOA bias current of 350 mA for high-gain operation, the timing jitter is greatly suppressed from 1.8 ps to 345 fs. Such a greatly suppressed timing

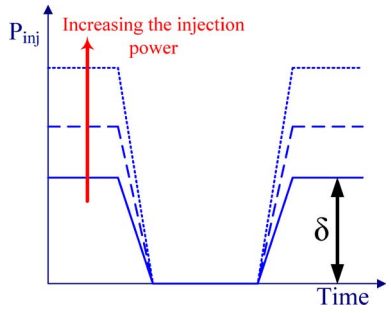


Fig. 7. Relationship between the injection power and the modulation depth.

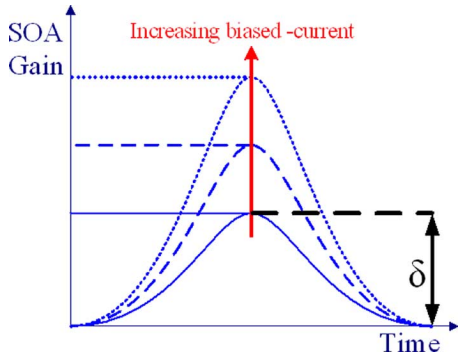


Fig. 8. Relationship between the gain of SOA and the modulation depth.

jitter is mainly attributed to the sufficiently high NRZ injection power, which effectively reduces the phase noise caused by the ASE in SOA.

In more detail, there is a tradeoff between the optical NRZ injecting level and the SOA bias current, which can be attributed to the empirical equation describing the relationship among the pulsewidth, gain, and modulation depth of mode-locking lasers [21], $\tau_p = (2\ln 2/\pi)^{1/2}[(2g_0/\delta^2)^{1/4}/({}_m\Delta\nu)^{1/2}]$, where $\tau_{\rm p}$ is the FWHM of the pulse, $g_0$ is the single-pass integrated gain, $f_m$ is the modulation frequency, $\delta$ is the modulation depth, and $\Delta\nu$ is the homogeneous linewidth. In general, the SOAFL with a lower gain and higher modulating depth facilitates the mode locking with a shorter pulsewidth. The modulation depth can definitely be enlarged by strong optical injection in our case; however, the residual gain must be sufficiently high to initiate mode-locking mechanism in SOAFL.

As illustrated in Figs. 7 and 8, these two parameters could compete with each other, and a compromised result can be done by increasing the duty cycle of the optical NRZ injection to limit the buildup of SOA gain at moderate level. With such an operation, the modulation becomes deeper and the residual gain of SOA remains sufficient to overcome the mode-locking threshold. According to the equation, the mode-locking pulsewidth should be broadened as the bias current of SOA detunes from 250 to 350 mA, whereas it is shortened oppositely due to the extremely deep modulation of SOA via the optical NRZ injection in our case. Therefore, we utilize the square dependency between the modulation depth and the pulsewidth to induce a highly gain-saturation condition of SOA for shortening the mode-locking SOAFL pulsewidth.

### *B. Optical Injection Induced Pulse-Plasma Interaction and Blueshifted Spectrum*

It is mandatory to realize the information the mode-locking spectrum and linewidth under such an optical NRZ injection prior to design the optimized dispersion compensation stage for shortening the mode-locked SOAFL pulses. By detuning the power of the optical NRZ data from $-3$ to 8 dBm, we also investigate the evolution of the ASE and mode-locking spectra of the SOAFL at different bias currents. Fig. 9 depicts the spectra of the mode-locking SOAFL at different NRZ injecting conditions and SOA bias currents. Two gain peaks from the SOAFL output are observed when the NRZ injection power is weak: one broadened peak at 1520 nm is generated by ASE and another at 1555.7 nm is due to the mode locking of SOAFL under NRZ injection. In Fig. 9(c), it is straightforward that the ASE spectrum of SOA becomes narrower at larger biases approaching self-lasing threshold condition, whereas the ASE spectrum is gradually broadened with increasing optical NRZ power as the ASE gain is diminishing far away from the self-lasing threshold condition. With increasing NRZ injecting power, the residual gain for the ASE at shorter wavelength is reduced; however, such a temporally modulated NRZ injection simultaneously facilitates the gain for mode locking the SOAFL at longer wavelength. That is, the SOAFL favors the mode-locking mechanism to survive in the fiber ring cavity with the assistance of a larger optical NRZ injection.

As a result, the mode locking supersedes the ASE to acquire most SOA gain that is built up within a narrow temporal window. The pulsed SOA gain is increased as the SOA current and the NRZ injection increase, and compromise each other. The original mode-locking SOA spectrum is redshifted by increasing the bias as well as the gain of SOA at constant NRZ injection power. At constant NRZ injection level, such a spectral redshift can be up to 5 nm by increasing the SOA bias from 250 to 350 nm, as shown in Fig. 10. In particular, the mode-locking mechanism still dominates the SOAFL with its spectrum slightly blueshifted. When increasing the NRZ injection power from $-3$ to 8 dBm, we have observed that the mode-locking SOAFL spectrum can be blueshifted from 1552 to 1548 nm, from 1555 to 1551 nm, and from 1557 to 1552 nm at SOA bias currents of 250, 300, and 350 mA, respectively.

This phenomenon is completely opposite to those observed in mode-locking lasers using other modulation techniques previously. In common sense, the residual gain of SOA at the strong injection condition is less than the weak injection condition. Our results reveal that the CW ASE is completely eliminated by strong NRZ injection, but the mode locking can still be obtained due to the residual SOA gain within in an extremely short time scale. At the very beginning, such an anomalous phenomenon is preliminarily attributed to the competition between ASE and mode-locking behaviors in the SOAFL at gain saturation condition. In principle, the relationship between wavelength peak of gain profile and upper level carrier density is given by the nonlinear gain compression effect described by $\lambda_n = \lambda_0 - \kappa_0(N - N_0)$ [22], where $\lambda_n$ is the shift of gain peak wavelength, $\lambda_0$ is the gain peak wavelength at transparency, $\kappa_0$ is a constant characterizing the gain peak shift, $N$ is the carrier concentration, and $N_0$ is the carrier density at transparency.

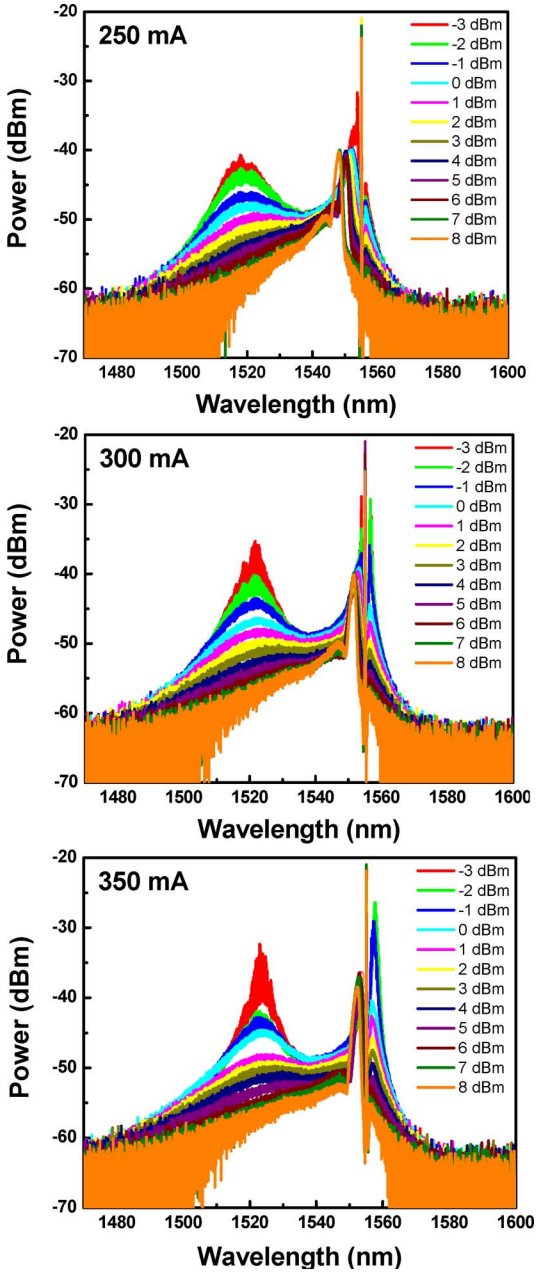


Fig. 9. Output spectra of the mode-locked SOAFL under different bias currents and NRZ injecting powers.

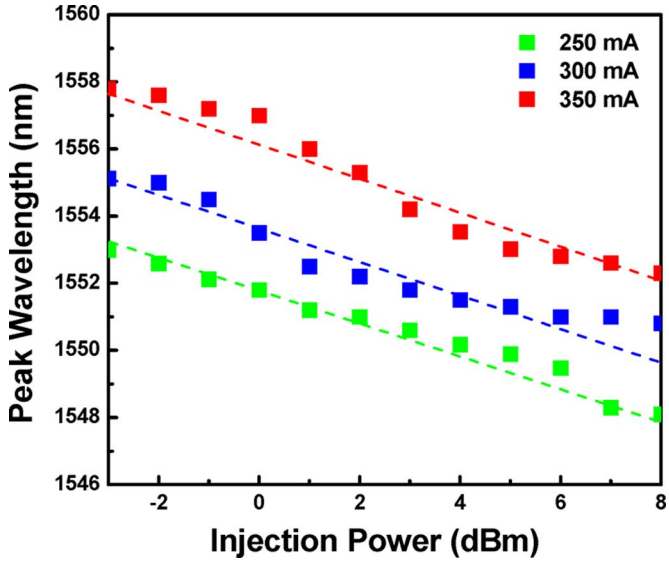


Fig. 10. Electron–hole plasma-induced wavelength blueshift of the mode-locking SOAFL pulse spectrum.

By operating the SOA at strong gain-saturation condition with increasing NRZ power, the ASE of SOA at 1520 nm is gradually eliminated, whereas the mode-locking gain peak arises and blueshifts from 1558 to 1552 nm due to band-filling effect at longer wavelength region. Such a blueshift in mode-locking spectrum becomes more significant in SOA at lower bias (or gain) condition. Previously, a similar phenomenon was observed with the intensity-dependent blueshift of the laser pulse spectrum up to 11 nm, which was attributed to the temporally asymmetric self-phase modulation in air-breakdown plasma region. Such a phenomenon can be manifested under intense light emission, while the electron–hole plasma is formed at the focused point within a high-power femtosecond dye amplifier [23]. Such a significant blueshift in the entire pulse spectrum is correlated with the negative refractive index ramp rapidly created by the ionized plasma, which was reported to be linearly proportional to the peak intensity of the laser pulse. In this case, the incident laser pulse will experience an enhanced frequency upshift when propagating through the region with a sufficiently large variation on refractive index in time domain. No matter the electrons are caused either by external source or the pulse itself, the plasma-induced spectral blueshift diminishes when the electrons are recombined or escaped from the interaction region within the pulse duration.

Instead of the gaseous media used in aforementioned works, semiconductors can be the alternative candidates to cause the plasma-induced spectral blueshift. Even a moderately intense laser pulse could transiently induce a large refractive index change by creating a dense electron–hole plasma within the carrier lifetime of hundreds picoseconds [24]. By technically keeping the pumping laser power far below the damage threshold, the accelerated decay dynamics of the plasma at high densities can be neglected to preserve a sufficiently large window in the time domain for the pulse-plasma interaction. The theory and numerical simulations on the interaction of ultrashort laser pulses with nonstationary electron–hole plasma in semiconductor was demonstrated by Berezhiani and coworkers, and the corresponding frequency upconversion was given by $\Delta\omega_0/\omega_0 \propto I_0(m_e\lambda_0^3/m_*\varepsilon_0^{1/2})$, where $\Delta\omega_0$ denotes the upshifted frequency, $I_0$ is the initial peak intensity of the laser pulse, $\lambda_0$ is the central wavelength of the laser pulse, $\varepsilon_0$ is the dielectric permittivity, and $m_e$ and $m_*$ are the mass and effective mass of electron in semiconductor, respectively. [25] In our case, such a transient electron–hole plasma also occurs by highly biasing the SOA and temporally saturating its gain with the incoming optical NRZ data stream. The circulated SOAFL pulse can thus interact with the electron–hole plasma induced by the free carriers with time-varied densities.

In Fig. 11, the peak spectral powers at bias current of 250, 300, and 350 mA are decreased from $-36$ to $-40.6$ dBm, from $-29$ to $-40$ dBm, and from $-27$ to $-38$ dBm, respectively,

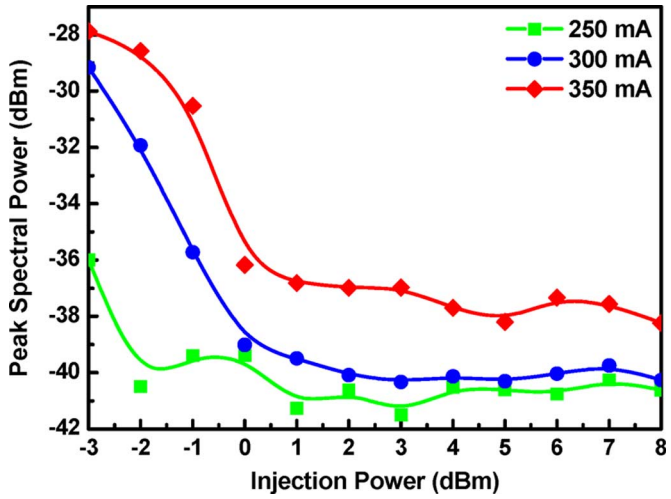


Fig. 11. Peak spectral power of SOAFL at different biases versus optical NRZ injection power.

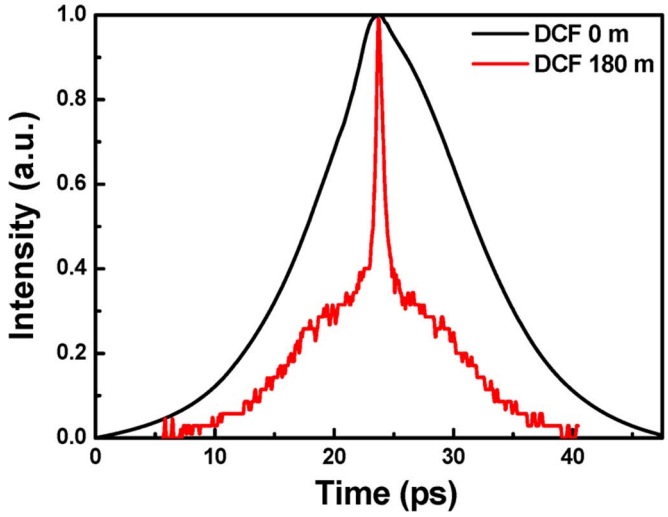


Fig. 13. Pulse comparison is between no compensation and compensation.

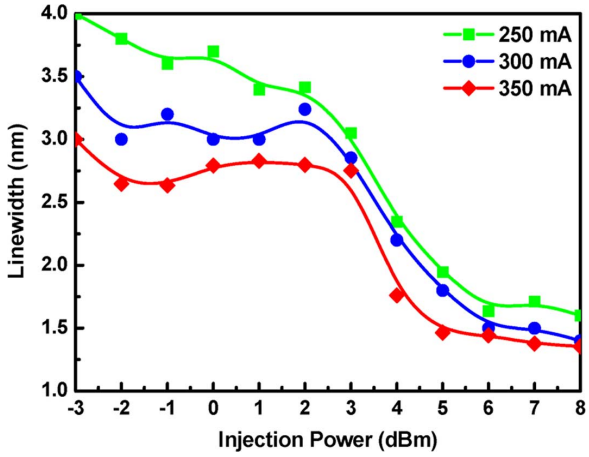


Fig. 12. Spectral linewidth of SOAFL at different biases versus optical NRZ injection power.

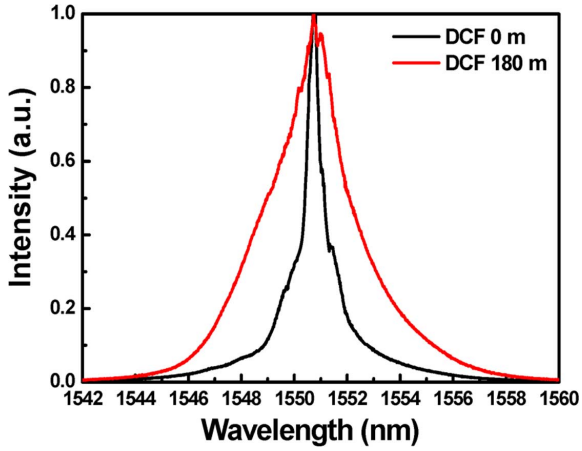


Fig. 14. Wavelength comparison is between no compensation and compensation.

due to the decreasing gain for mode locking the SOAFL with increasing NRZ injection power. Moreover, we have also observed the reduction on spectral linewidth of the mode-locking SOAFL with increasing optical NRZ power, as shown in Fig. 12. Both the original 3-dB spectral linewidth and the corresponding dynamic range [defined as $(\lambda_{\text{high}} - \lambda_{\text{low}})/\lambda_{\text{high}}$] of the optical NRZ injection-mode-locked SOAFL shrink with enlarging SOA bias current. By increasing the SOA current from 250 to 350 mA, the linewidth and dynamic range is decreases by 1 nm (from 4 to 3 nm) and 20% (from 65% to 45%). The linewidth reduction accompanied with the frequency upshifting result is relatively in good agreement with that ever obtained in the dye and gaseous pulse-plasma interaction system, [23] indicating that the strong NRZ injection power effectively saturates the gain of SOA to produce a sufficiently large refractive index change under the existence of high-density electron–hole plasma.

As evidence, the enhanced electron–hole plasma under strong NRZ injection can also be confirmed with the observation on the reducing CW gain of SOA in terms of the decreasing dc levels at the output pulse, as illustrated in Fig. 4. In Figs. 4 and 13, we demonstrate that the strong NRZ injection power prevents the ASE generating and optimizes the mode locking condition. After propagating through an EDFA, we investigate the dispersion compensation results of the mode-locked SOAFL pulse by using the dispersion-compensated fiber (DCF) with its length detuning from 20 to 200 m. Before compensation, the pulsewidth and linewidth of SOAFL after EDFA is 11 ps and 1 nm, respectively. After compensation, the pulsewidth of SOAFL is shortened to 836 fs with its linewidth broadened to 3 nm, as shown in Figs. 12 and 13. In Fig. 14, the broadened linewidth of SOAFL is probably due to the EDFA amplification induced nonlinear self-phase modulation effect, which causes the SOAFL spectrum to slightly broadened from 1 to 3 nm. The extremely small duty cycle of 0.8% and the moderate spectral linewidth of 3 nm for one bit of the recovered RZ clock pulse are obtained after dispersion compensation.

After dispersion compensation, the recovered RZ clock pulse reaches nearly transform-limit condition with a time-bandwidth product of 0.314. Note that the compensation process is somewhat incomplete and leaves a pedestal associated with the central pulse peak of the SOAFL (see Fig. 13). The spectral broadening is attributed to the self-phase modulation effect. [1] Be-

fore dispersion compensation, the SOAFL pulse does not enter the Fourier transform-limited regime. That is, the time-bandwidth product of the original SOAFL pulse is not transform-limited with a constant value of 0.31 (hyperbolic second-like pulse shape) or 0.44 (Gaussian-like pulse shape). The pulse shortening is happened due to the compensation between the SOAFL pulse chirp and the group velocity dispersion when propagating in fiber. In principle, there should not be any spectral broadening effect occurred during such a linear dispersion stage. Only when the nonlinear effect such as self-phase modulation occurs, the SOAFL pulse spectrum becomes broadened. It seems that some nonlinear chirping effect has been initiated during the amplification and propagation of the mode-locked SOAFL pulses in EDFA and DCF. This is confirmed from the broadened spectrum on the amplified and compensated pulses. Those chirped frequency components in the amplified SOAFL pulses exhibit different amplitudes, which are unable to be linearly compensated in DCF.

## IV. Conclusion

By detuning the bias current of SOA from 250 to 350 mA and the power level of the optical NRZ injection from $-3$ to 8 dBm, we investigate the 10-GHz mode locking and pulsed clock extraction from an SOA-based fiber ring injected by optical NRZ data at 10 Gbit/s. With increasing NRZ power, the ASE at 1520 nm is eliminated and the SOA leaves more gain for initiating the mode locking. The strong injection can effectively decrease the dc level of the recovered RZ clock pulse and eliminates its timing jitter to 600 fs. The mode locking is gradually completed with the dc level greatly decreasing from 480 to 50 $\mu$W, corresponding to a pulse/dc amplitude contrast ratio up to 18 dB. By increasing the bias current to 350 mA and the NRZ injection power to 8 dBm for operating the SOA at high-gain and high-modulation-depth conditions, the extracted mode-locking pulsewidth can be shortened from 55 to 27 ps and the timing jitter is greatly suppressed from 1.8 ps to 345 fs. The gain and intracavity power detuned anomalous subpicosecond timing jitter, and blueshifted mode-locking spectrum are elucidated with theoretical models and empirical equations. The mode-locked SOA spectrum is redshifted by 5 nm with increasing bias as well as gain of SOA at constant NRZ injection level. Nonetheless, the mode-locking gain peak arises and blueshifts from 1558 to 1552 nm due to electron–hole plasma-induced band-filling effect. The anomalous blueshift in mode-locking SOAFL spectrum is mainly attributed to the effect of nonlinear gain compression of ASE in SOA with a transient gain saturation effect. Such a blueshift in mode-locking spectrum becomes more significant in SOA at lower bias (or gain) condition. With optimized NRZ injection power and SOA bias current, the EDFA-amplified SOAFL pulsewidth can be shortened from 11 ps to 836 fs after the dispersion compensation.

## References


[1] P. G. J. Wigley, A. V. Babushkin, J. I. Vukusic, and J. R. Taylor, "Active mode locking of an erbium-doped fiber laser using an intracavity laser diode device," *IEEE Photon. Technol. Lett.*, vol. 2, no. 8, pp. 543–545, Aug. 1990.

[2] D. Bums and W. Sibbert, "Controlled amplifier modelocked Er3+ fiber ring laser," *Electron. Lett.*, vol. 26, no. 8, pp. 505–506, Apr. 1990.

[3] K. Smith, J. R. Annitage, R. Wyatt, N. J. Doran, and S. M. J. Kelly, "Erbium fiber soliton laser," *Electron. Lett.*, vol. 26, no. 15, pp. 1149–1151, Jul. 1990.

[4] K. Tamura, H. A. Haus, and E. P. Ippen, "Self-starting additive pulse mode-locked erbium fiber ring laser," *Electron. Lett.*, vol. 28, no. 24, pp. 2226–2227, Nov. 1992.

[5] V. J. Matsas, W. H. Loh, and D. J. Richardson, "Self-starting, passively mode-locked Fabry–Perot fiber soliton laser using nonlinear polarization evolution," *IEEE Photon. Technol. Lett.*, vol. 5, no. 5, pp. 492–494, May 1993.

[6] N. V. Pedersen, K. B. Jakobsen, and M. Vaa, "Mode-locked 1.5 $\mu$m semiconductor optical amplifier fiber ring," *OSA/IEEE J. Lightw. Technol.*, vol. 14, no. 5, pp. 833–838, May 1996.

[7] T. Papakyriakopoulos, K. Vlachos, A. Hatziefremidis, and H. Avramopoulos, "20-GHz broadly tunable and stable mode-locked semiconductor amplifier fiber ring laser," *Opt. Lett.*, vol. 24, no. 17, pp. 1209–1211, Sep. 1999.

[8] E. J. Greer, Y. Kimura, K. Suzuki, E. Yoshida, and M. Nakazawa, "Generation of 1.2 ps, 10 GHz pulse train from all-optically mode locked, erbium fibre ring laser with active nonlinear polarization rotation," *Electron. Lett.*, vol. 30, no. 21, pp. 1764–1765, Oct. 1994.

[9] W. H. Cao and K. T. Chan, "Generation of bright and dark soliton trains from continuous-wave light using cross-phase modulation in a nonlinear-optical loop mirror," *IEEE J. Quantum Electron.*, vol. 37, no. 5, pp. 725–732, May 2001.

[10] J. He and K. T. Chan, "All-optical actively mode locked fibre ring laser based on cross-gain modulation in SOA," *Electron. Lett.*, vol. 38, no. 24, pp. 1504–1505, Nov. 2002.

[11] P. G. J. Wigley, A. V. Babushkin, J. I. Vukusic, and J. R. Taylor, "Active mode locking of an erbium-doped fiber laser using an intracavity laser diode device," *IEEE Photon. Technol. Lett.*, vol. 2, no. 8, pp. 543–545, Aug. 1990.

[12] J. N. Maran, S. LaRochelle, and P. Besnard, "Erbium-doped fiber laser simultaneously mode locked on more than 24 wavelengths at room temperature," *Opt. Lett.*, vol. 28, no. 21, pp. 2082–2084, Nov. 2003.

[13] D. M. Patrick, "Modelocked ring laser using nonlinearity in a semiconductor laser amplifier," *Electron. Lett.*, vol. 30, no. 1, pp. 43–44, Jan. 1994.

[14] D. H. Kim, S. H. Kim, Y. M. Jhon, S. Y. Ko, J. C. Jo, and S. S. Choi, "Relaxation-free harmonically mode-locked semiconductor-fiber ring laser," *IEEE Photon. Technol. Lett.*, vol. 11, no. 5, pp. 521–523, May 1999.

[15] D. Abraham, R. Nagar, M. N. Ruberto, G. Eisenstein, U. Koren, J. L. Zyskind, and D. J. Digiovanni, "Frequency tuning and pulse generation in a fiber laser with an intracavity semiconductor active filter," *IEEE Photon. Technol. Lett.*, vol. 5, no. 4, pp. 377–379, Apr. 1993.

[16] P. G. J. Wigley, A. V. Babushkin, J. I. Vukusic, and J. R. Taylor, "Active mode locking of an erbium-doped fiber laser using an intracavity laser diode device," *IEEE Photon. Technol. Lett.*, vol. 2, no. 8, pp. 543–545, Aug. 1990.

[17] E. Tangdiongga, J. P. Turkiewicz, G. D. Khoe, and H. de Waardt, "Clock recovery by a fiber ring laser employing a linear optical amplifier," *IEEE Photon. Technol. Lett.*, vol. 16, no. 2, pp. 611–613, Feb. 2004.

[18] A. Fernandez, L. Chao, and J. W. D. Chi, "All-optical clock recovery and pulse reshaping using semiconductor optical amplifier and dispersion compensating fiber in a ring cavity," *IEEE Photon. Technol. Lett.*, vol. 20, no. 13, pp. 1148–1150, Jul. 2008.

[19] G.-R. Lin, I. H. Chiu, and M. C. Wu, "1.2-ps mode-locked semiconductor optical amplifier fiber laser pulses generated by 60-ps backward large-duty-cycle comb injection and soliton compression," *Opt. Exp.*, vol. 13, no. 3, pp. 1008–1014, Feb. 2005.

[20] G.-R. Lin, Y. S. Liao, and G. Q. Xia, "Dynamics of optical backward-injection-induced gain-saturation modulation and mode locking in semiconductor optical amplifier fiber lasers," *Opt. Exp.*, vol. 12, no. 10, pp. 2017–2026, May 2004.

[21] J. T. Verdeyen, *Laser Electronic*, 2nd ed. Englewood Cliffs, NJ: Prentice-Hall, 1994, ch. 9.

[22] I. D. Henning, M. J. Adams, and J. V. Collins, "Performance prediction from a new optical amplifier model," *IEEE J. Quantum Electron.*, vol. 21, no. 6, pp. 609–613, Jun. 1985.

[23] W. M. Wood, G. Focht, and M. C. Downer, "Tight focusing and blue shifting of millijoule femtosecond pulses from a conical axicon amplifier," *Opt. Lett.*, vol. 13, no. 11, pp. 984–986, Nov. 1988.

[24] V. I. Berezhiani, S. M. Mahajan, and R. Miklaszewski, "Multiple reflections: Cascaded upshifting of laser pulses by semiconductors," *J. Opt. Soc. Amer. B, Opt. Phys.*, vol. 18, no. 5, pp. 617–622, May 2001.

[25] V. I. Berezhiani, S. M. Mahajan, and R. Miklaszewski, "Frequency up-conversion and trapping of ultrashort laser pulses in semiconductor plasmas," *Phys. Rev. A, Gen. Phys.*, vol. 59, no. 1, pp. 859–864, Jan. 1999.

[26] G. P. Agrawal and N. A. Olsson, "Self-phase modulation and spectral broadening of optical pulses in semiconductor laser amplifiers," *IEEE J. Quantum Electron.*, vol. 25, no. 11, pp. 2297–2306, Nov. 1989.

**Gong-Ru Lin** (S'93–M'96–SM'04) received the Ph.D. degree in electrooptical engineering from the National Chiao Tung University, Hsinchu, Taiwan, in 1996.

He is currently the Director of the Laboratory of Fiber Laser Communications and Si Nano-Photonics, Graduate Institute of Photonics and Optoelectronics, and the Department of Electrical Engineering, National Taiwan University, Taipei, Taiwan. He has authored or coauthored more than 140 papers in SCI cited international journals. His research interests include femtosecond fiber lasers, nanocrystallite Si photonics, all-optical data processing, and millimeter-wave photonic phase-locked loops.

Prof. Lin is a member of the Optical Society of America and a Fellow of the International Society for Optical Engineers. He is currently the Vice Chair of the IEEE/Laser and Electro-Optics Society Taipei Chapter.

**Yu-Chan Lin** was born in Kaohsiung, Taiwan, in 1981. He received the B.S. degree in physics from Soochow University, Taipei, Taiwan, in 2007, and the M.S. degree in engineering from the Institute of Electro-Mech-Optic Engineering, China Institute of Technology, Guangzhou, China. Currently, he working toward the Ph.D. degree in the Graduate Institute of Photonics and Optoelectronics, and the Department of Electrical Engineering, National Taiwan University, Taipei.

His research interests include mode-locked semiconductor optical amplifier fiber laser.

**Kuen-Cherng Lin,** photograph and biography not available at the time of publication.

**Guo-Hsuan Peng** received the B.S. and M.S. degrees in mechanical engineering and photonics and optoelectronics from the National Taiwan University, Taipei, Taiwan, in 2006 and 2008, respectively.

He is currently with the Graduate Institute of Photonics and Optoelectronics, and the Department of Electrical Engineering, National Taiwan University, Taipei, Taiwan. His research interests include the mode locking and soliton compression of semiconductor optical amplifier-based fiber lasers and theirs application in dense wavelength-division multiplexing networks.